Liquid Crystals
Publication details, including instructions for authors and subscription information:
http://www.informaworld.com/smpp/title~content=t713926090

Spontaneous polarization and electro-optic behaviour of a ferroelectric liquid crystal cell fabricated with polyimide Langmuir-Blodgett films

Hyun-Wuk Kim; Hyun-Sang Lee; Jong-Duk Kim

To cite this Article Kim, Hyun-Wuk , Lee, Hyun-Sang and Kim, Jong-Duk(2002) 'Spontaneous polarization and electro-optic behaviour of a ferroelectric liquid crystal cell fabricated with polyimide Langmuir-Blodgett films', Liquid Crystals, 29: 3, 413 — 420

To link to this Article: DOI: 10.1080/02678290110104595

URL: http://dx.doi.org/10.1080/02678290110104595

Liquid Crystals, 2002, Vol. 29, No. 3, 413–420

Taylor & Francis
Taylor & Francis Group

Spontaneous polarization and electro-optic behaviour of a ferroelectric liquid crystal cell fabricated with polyimide Langmuir–Blodgett films

HYUN-WUK KIM, HYUN-SANG LEE and JONG-DUK KIM*
Department of Chemical Engineering,
Korea Advanced Institute of Science and Technology, Taejon, 305-701, Korea

(*Received 23 February 2001; in final form 21 June 2001; accepted 24 September 2001*)

The spontaneous polarization and electro-optic response of ferroelectric liquid crystals (FLCs) were investigated in a cell fabricated with a polyimide alignment layer coated by the Langmuir–Blodgett method. The surface properties of the cured polyimide layers were monitored by contact angle measurement, and by FTIR spectroscopy and AFM for the orientation and surface roughness, respectively. The apparent spontaneous polarization of an FLC determined in a practical sandwich-cell depended on various conditions such as cell thickness, cooling rate from the smectic A to chiral smectic C phase, and deposition pressure. Electro-optic response and decay times of FLCs were also measured. Furthermore, the ions in the FLC mixture reduced the magnitude of the effective electric field, but had no effect at high frequency.

1. Introduction

The alignment layer of surface-stabilized ferroelectric liquid crystal displays (SSFLCs) has generally been fabricated by rubbing a polyimide (PI) film, but the electrostatic damage on the thin film transistor and dust contamination limits process yields in industry [1]. Therefore, alternative alignment methods such as obliquely evaporated SiO films [2] and Langmuir–Blodgett (LB) films [3], whose anchoring strength was estimated to be weak in the nematic phase [4], have been investigated.

In general, the anchoring force of an alignment layer has a significant effect on the switching of liquid crystals [5]. It is expected that if the surface anchoring strength is weak, FLC molecules on or near the surface could switch smoothly to realize uniform switching. Therefore, the characteristics of PI alignment layers with different treatments such as rubbing strength, cooling rate and field application, have previously been investigated by observing the dynamic behaviour of LFCs under electric fields [6].

In this work, we report the spontaneous polarization and optical response of FLCs in cells fabricated under varying conditions with an LB film alignment layer whose anchoring force is weak; the optimal conditions for electro-optic response of the FLC cells is destined by observing the switching of the cells.

2. Experimental

Alignment layers with weak anchoring force were deposited on the ITO-coated glass and transferred with a KSV 5000 instrument (KSV Instrument Ltd., Finland) from a Langmuir monolayer. The available maximum and minimum areas of the trough were 85 000 and 14 400 mm^2, respectively. The surface pressures of the monolayer at the air–water interface were determined with a sand-blasted platinum plate, its dynamic range and resolution being 0–100 mN m^{-1} and 4 μN m^{-1}, respectively.

Poly(amic acid) was used as the polyimide precursor and was prepared from pyromellitimide dianhydride (PMDA-ODA), see figure 1. It is hydrophilic and soluble in water and therefore cannot form a monolayer at the air–water interface. Hexadecylamine (DMC 16) was attached to poly(amic acid) as the alkylamine salt [7] and gave sufficient hydrophobicity for the polymer to form a stable monolayer. *N*,*N*′-dimethylformamide (DMF) was used as the solvent for the poly(amic acid) alkylamine salt (PAAS) to be spread on the purified water. The solution (70 ml) was spread on the pure water subphase obtained from a Milli-Q purification system (18.2 mΩ cm^{-1}); no significant solvent effects were observed. The temperature of the subphase was controlled by circulating water through a pipe attached to the LB trough.

---

*Author for correspondence; e-mail: kjd@kaist.ac.kr

Liquid Crystals ISSN 0267-8292 print/ISSN 1366-5855 online © 2002 Taylor & Francis Ltd
http://www.tandf.co.uk/journals
DOI: 10.1080/02678290110104595

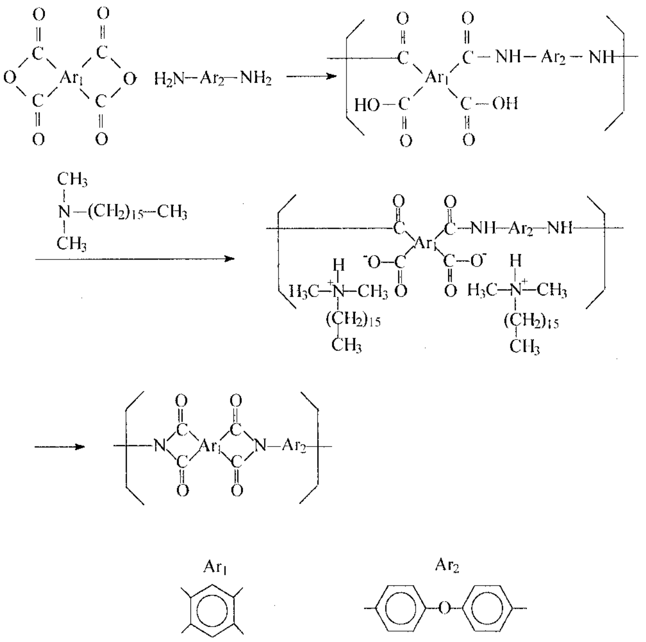

Figure 1. Synthetic route to the polyimide.

The LB films were built up at a speed of 5 mm min^{-1} on ITO-coated glass ($40 \times 15 \times 0.7\,\mathrm{mm}^3$) for a sample cell and a Si wafer ($50 \times 13 \times 1\,\mathrm{mm}^3$) for either AFM or FTIR spectroscopic studies. The substrate dipping was delayed for 360 s after the up-stroke in air and for 60 s after the down-stroke in the subphase. All substrates were cleaned with acetone and chloroform before deposition, and rinsed using deionized-water and dried for 30 min in a vacuum oven at 50°C. The deposition of PAAS on the substrate was performed at surface pressures of 5, 15, 25 and 35 mN m^{-1} and at a barrier speed of 4 mm min^{-1}. The films of PMDA-3,3′-ODA PAAS were cured at 300°C for 1 h [8] to yield the polyimide; the synthetic path is shown in figure 1.

Contact angles of water on the alignment layers at various curing temperatures were measured using the G403 Contact Angle Measuring System (Marktech Co.). The 5-layers samples were prepared at 30 mN m^{-1} and cured at 200, 250, 300, 350 and 400°C.

FTIR absorption spectra were measured using a FTS-60 spectrometer with deuterated triglycine sulfate (DTGS). For all the absorption measurement, 50 spectral scans were averaged with a 4 cm^{-1} resolution.

The surface roughness was determined with AFM images for a number of layers on a Si wafer. AFM images were obtained using an AutoProbe M5 (Park Scientific Ins., USA) in non-contact mode. The structure of the FLC cell used was a sandwich-type, having FLCs inserted between two ITO-glass substrates coated with polyimide alignment layers. Polyethylene terephthalate (PET) film with a thickness of 2, 7.5 or 12 µm was inserted between the two substrates as a spacer. After the deposition of a film onto the ITO-glass, adhesive (Mitsui Toatsu Chem. Inc., Japan) was used to fix the two substrates in a parallel configuration. A FLC mixture, ZLI-4654-100 (Merck), was injected into an empty cell in the isotropic phase and cooled to the smectic phase. The phase sequence of this material is:

$$\mathrm{SmC}^* \underset{61^\circ\mathrm{C}}{-} \mathrm{SmA} \underset{65^\circ\mathrm{C}}{-} \mathrm{N}^* \underset{74^\circ\mathrm{C}}{-} \mathrm{I}$$

The spontaneous polarization of FLCs in the cell was measured by the triangular wave method [9, 10]. Symmetric triangular waves of frequency 10 Hz and with 5, 6, 7, 8, 9, 10, 15 or 20 $V_{p\text{-}p}$ were applied by a programmable function generator, HM 8130. The current was measured by the voltage drop across a standard resistor, and the signal was recorded using a personal computer via an AD converted and HP 5461B oscilloscope. The response time was measured by applying various symmetric square pulse waves and the decay time using a biased square wave of 10 Hz and 20 ms pulse width [10].

3. Results and discussion

3.1. *Film deposition and orientation of polyimide*

The π–A isotherm of PAAS at 25°C (see figure 2) showed the stable monolayer at the air–water interface with a collapse pressure of 45 mN m^{-1} [11]. The phase transition from less dense to a packed state was observed at the limiting area of 140 Å^2/molecule and beyond that the surface pressure steeply increased. The longer the alkyl chain length of PMDA-3,3′-ODA, the more stable

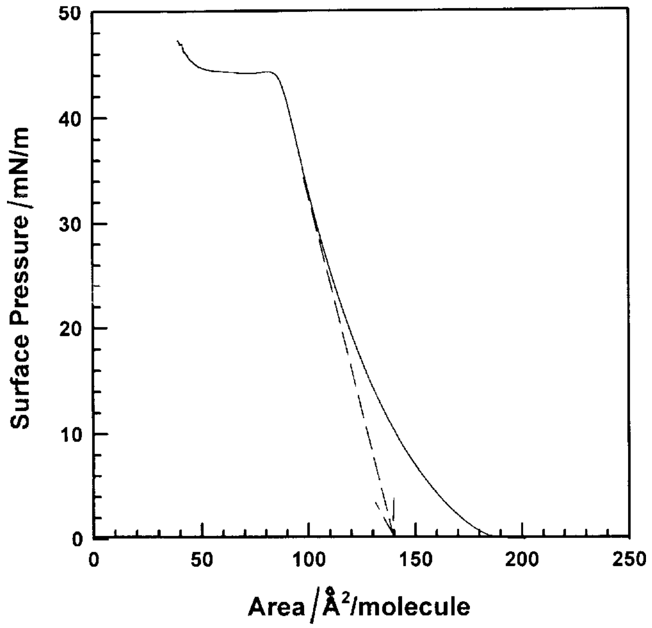

Figure 2. π–A isotherm of PMDA-3,3′-ODA PAAS at 25°C.

are the monolayers. In deposition, the transfer type is transformed from the Y-type to the Z-type, and better transferability was observed at the stable monolayer [11].

Figure 3 shows the transfer characteristics of PMDA-3,3′-ODA PAAS onto ITO-glass at different surface pressures and at a dipping speed of 5 mm min^{-1}. Deposition of 35 mN m^{-1} always showed the Y-type, while at 25 mN m^{-1} the initial three strokes showed the Y-type but changed to the Z-type at four strokes and beyond. However, the films transferred at 5 and 15 mN m^{-1} showed the Z-type and partial peel-off. Therefore, we conclude that the more stable monolayers of PAAS were formed at high surface pressures and these had the better transfer characteristics.

In FTIR spectroscopy, the electric dipole transition moment for the 1240 cm^{-1} band exists along the molecular axis; the moment for the 1720 cm^{-1} band is perpendicular to the molecular axis. The intensity difference between spectra parallel and perpendicular to the dipping direction contains information about the structure induced by the dipping process. The band at 1240 cm^{-1} is highly polarized along the dipping direction, whereas the band at 1720 cm^{-1} is enhanced perpendicularly to the dipping direction. The in-plane orientations of PAAS and the polyimide LB films were determined by plotting the absorbance of the 1240 and 1720 cm^{-1} bands against the rotation angle. Figure 4 shows that C–O–C band (1240 cm^{-1}, parallel to the molecular axis) has a maximum in the direction parallel to dipping while the C=O band (1720 cm^{-1}, perpendicular to molecular axis) has a minimum in the direction parallel to dipping [12]. This result indicates that the polymer chains in the PMDA-3,3′-ODA PAAS and polyimide are aligned to the dipping direction, and the orientations of PMDA-3,3′-ODA PAAS and polyimide are almost the same.

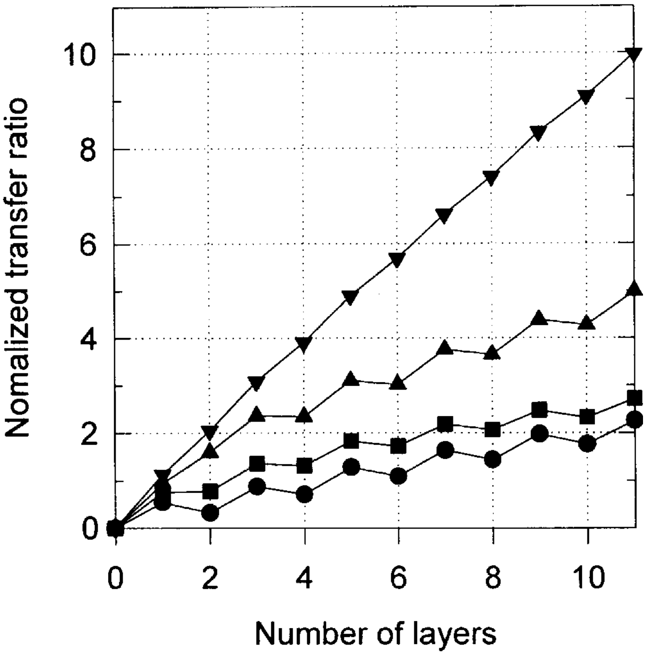

Figure 3. Normalized transferred area of PMDA-3,3′-ODA PAAS onto ITO-glass at various surface pressures; ● 5, ■ 15, ▲ 25, ▼ 35 mN m^{-1}.

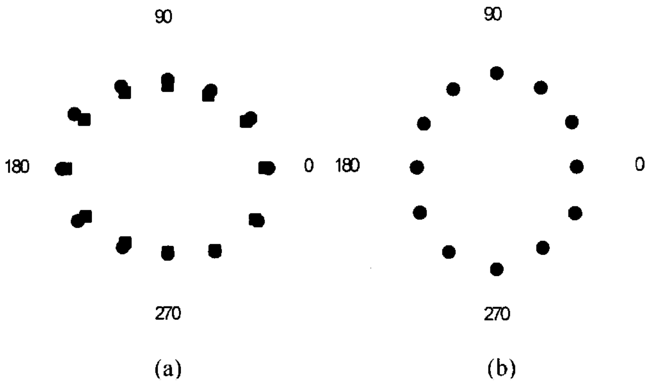

Figure 4. Polarization angle dependence of (*a*) the 1240 cm^{-1} band (C–O–C, parallel to the molecular axis) and (*b*) the 1720 cm^{-1} band (C=O, perpendicular to the molecular axis). The polarization angle is 0° and 180° when the polarization of the IR beam is parallel to the deposition direction. The circle is PMDA-3,3′-ODA PAAS; the square is polyimide.

3.2. *Surface characteristics of the PI LB film*

The contact angle was measured using the Contact Angle Meter (Marktech Co.), with deionized water as a drain; ten tests were performed per sample. Figure 5 shows the contact angles at different curing temperatures. The polar component of the surface energy is related to the atom percentage of the polar groups, and the polar groups such as oxygen and nitrogen in poly(amic acid) will be exposed on the surface at low degrees of imidization [6]. At high temperatures, however, poly(amic acid) is rapidly imidized to the polyimide. Thus, few polar groups exist on the film and it therefore becomes more hydrophobic.

AFM images of PI LB films on Si wafers were observed for various deposited layer numbers. As the layer number increased, the film surface became increasingly smooth because it was sufficiently thick to cover the original roughness of the Si wafer substrate. Figure 6 shows that the rms roughness decreased rapidly with the first deposition layer and gradually saturated thereafter.

3.3. *Tilt angle and spontaneous polarization of FLCs*

The optical switching of the FLC was performed between two stable positions of small angular difference in the plane. Half this angle is defined as the ‘tilt

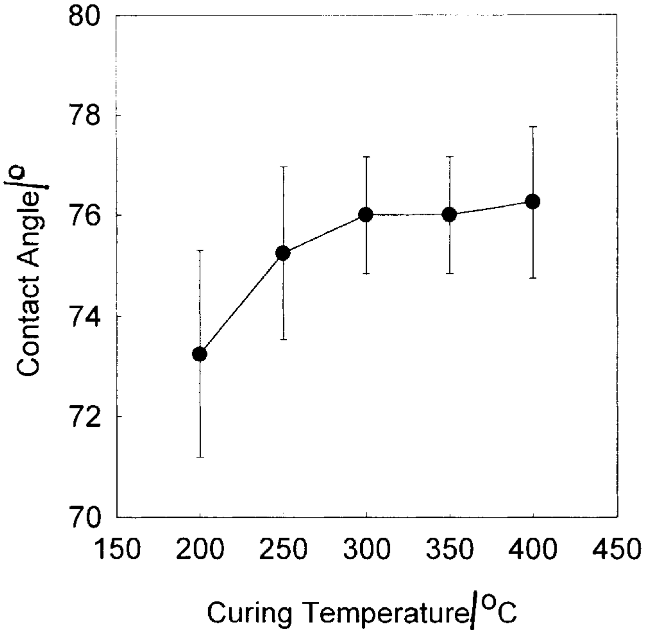

Figure 5. Dependence of contact angle on curing temperature.

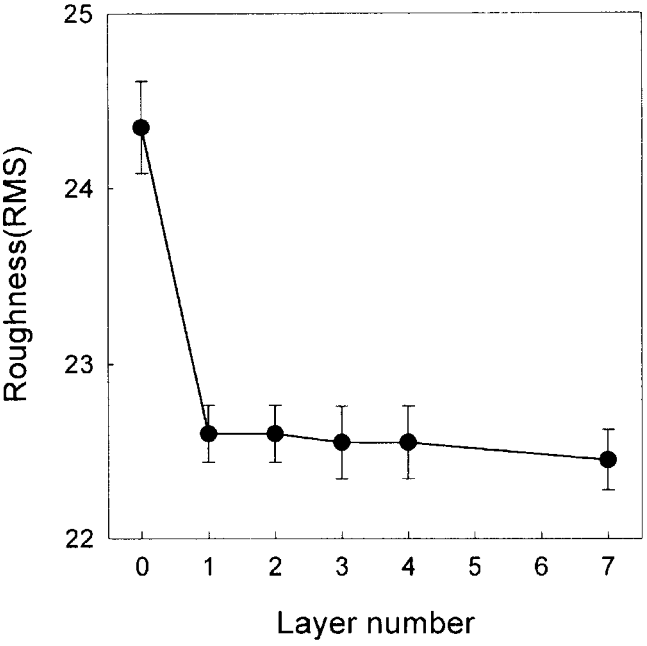

Figure 6. The rms roughness of a polyimide LB alignment layer on a Si wafer.

angle', determined by the sample rotation method [13]. Figure 7 shows the FLC tilt angles in the chiral smectic C phase. The tilt angle decreases as the temperature approaches the chiral smectic C to smectic A transition temperature. The increase in the tilt angle was very sharp within the range of the initial 10°C from the

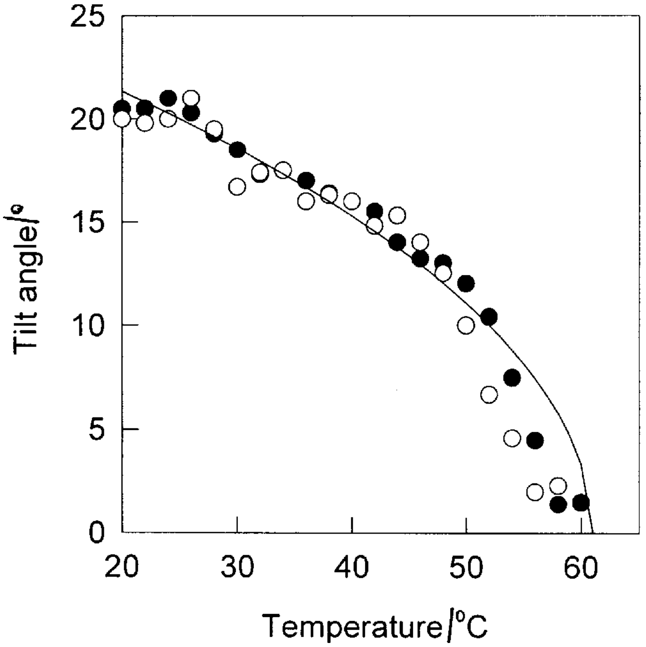

Figure 7. FLC tilt angle in a 2 μm thick cell, measured during heating (filled circle) and cooling (open circle). Solid line represents the theoretical value obtained using the Landau equation.

transition temperature and became smooth beyond this range. The solid line in figure 7 represents theoretically calculated angles of power law dependence [14].

$$\theta(T) = \theta_0 (T_c - T)^{\beta}$$

where θ is the tilt angle at temperature T (°C), θ_0 is the proportionality constant, T_c is the transition temperature from chiral smectic C to smectic A, T is the actual temperature, and theoretically the exponent β should have a value of 0.5.

The switching behaviour of a FLC under electric fields depends on its physical properties and alignment states. In a circuit analysis, the FLC cell is regarded as a parallel combination of a resistor (R), a capacitor (C), and a polarization reversal device [9, 15]. When various electrical function waves are applied to the FLC cell, its response current can be derived as follows,

$$I = I_c + I_i + I_p = C(\mathrm{d}V/\mathrm{d}t) + V/R + \mathrm{d}P/\mathrm{d}t$$

where I is the induced current, I_c is the charge accumulation, I_i is the current by an external field, I_p is the polarization realignment current, V is the applied voltage, and P is the amount of charge induced by the polarization realignment.

The spontaneous polarization under a switching current was measured to observe the FLC alignment states. The local spontaneous polarization of each domain in the FLC cell would be different as the orientations of the dipoles are different [14]. The domains of different polarization have different switching behaviour in the field, and therefore it is expected that a well aligned structure will respond easily to the field. Figure 8 shows the spontaneous polarization of FLC cells under different applied voltages. The alignment layers of the cells were prepared with the deposition at different surface pressures, and the liquid crystals were aligned under a cooling rate of 0.2°C min^{-1}. The spontaneous polarization significantly increases as the surface pressure increases at low applied field. At low fields, the switching behaviour of FLCs depends significantly on the surface conditions, while, at high fields, the surface force is negligible. This is consistent with results from the spontaneous polarization of cells prepared at different cooling rates. At a slow cooling rate, molecules are well aligned and polarized [8].

Figure 9 shows the spontaneous polarization of the chiral smectic C phase at various temperatures. As the temperature approaches the chiral smectic C to smectic A transition, the switching behaviour becomes insensitive and finally disappears. It is reported that the layer spacing and the tilt angle of FLC molecules to the layer direction in a chiral smectic C phase decreases as the temperature increases [14, 16]. The solid line represents the power law expression of the spontaneous polarization,

$$\mathbf{P}_S(T) = \mathbf{P}_{S0}(T_C - T)^{\alpha}$$

where $\mathbf{P}_S$ is the spontaneous polarization at temperature T (°C), $\mathbf{P}_{S0}$ is the proportionality constant, T_C is the transition temperature, T is the temperature at which the measurements are made, and theoretically, the exponent α is 0.5. The thick cells showed low spontaneous polarization and both the 7.5 and 12 μm thick cells have a typical focal-conic structure, while the 2 μm thick cell had the better alignment state. The FLC molecules in the thicker cell have a strong helical structure because of the weak surface force.

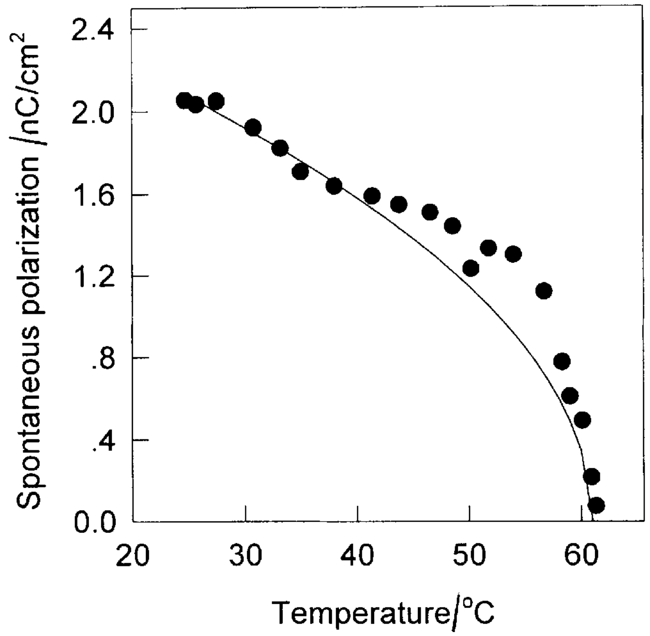

Figure 9. Spontaneous polarization of the chiral smectic C phase.

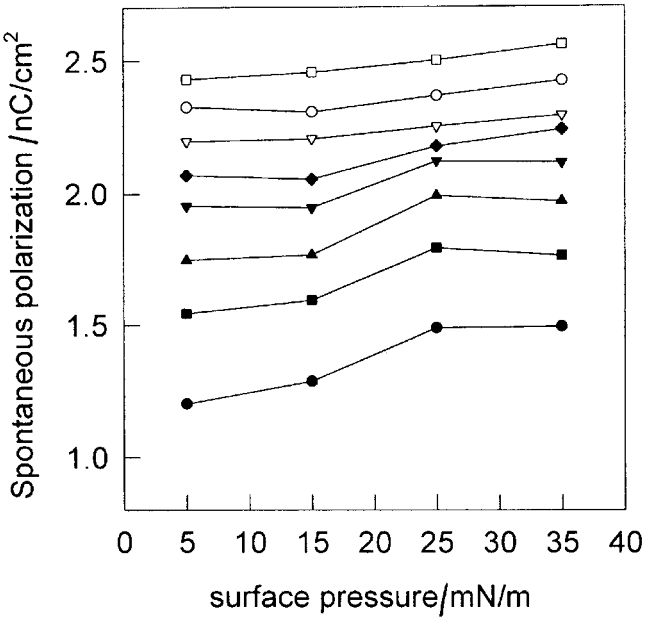

Figure 8. Spontaneous polarization of the FLC on PI LB film; 2 μm thick cell, 25°C; ● 5, ■ 6, ▲ 7, ▼ 8, ◆ 9, ▽ 10, ○ 15, 20 $V_{\mathrm{p\text{-}p}}$.

Figure 10 shows the spontaneous polarization of FLCs on the rubbed PI film. $\mathbf{P}_S$ increased with the rubbing strength and with the amplitude of the applied voltage. Rubbing strength can be defined as [17]:

$$L = Nl(1 + 2\pi rn/60v)$$

where N is the cumulative number of rubbings, l is the contact length of the circumference of the rubbing roller, n is the number of revolutions per minute (rpm) of the roller, r is its radius, and v is the velocity of the substrate stage. In our experiment, the rubbing conditions on the spin-coated alignment layer were fixed at $v = 0.7\,\mathrm{cm\,s}^{-1}$, $l = 0.2\,\mathrm{cm}$, $r = 6\,\mathrm{cm}$, $N = 1$ and $n = 54$, 280, 870 and 1250 rpm, i.e. $L = 10$, 50, 150 and 250. The switching current on the rubbed PI film is about 1.5–2 times larger than that on the PI LB film. In the rubbed cell, the alignment state of the molecules depends on the rubbing strength; so, as the rubbing strength increases, the spontaneous polarization also increases. In the case of rubbed cells, we obtained good alignment for rubbing strengths over 50.

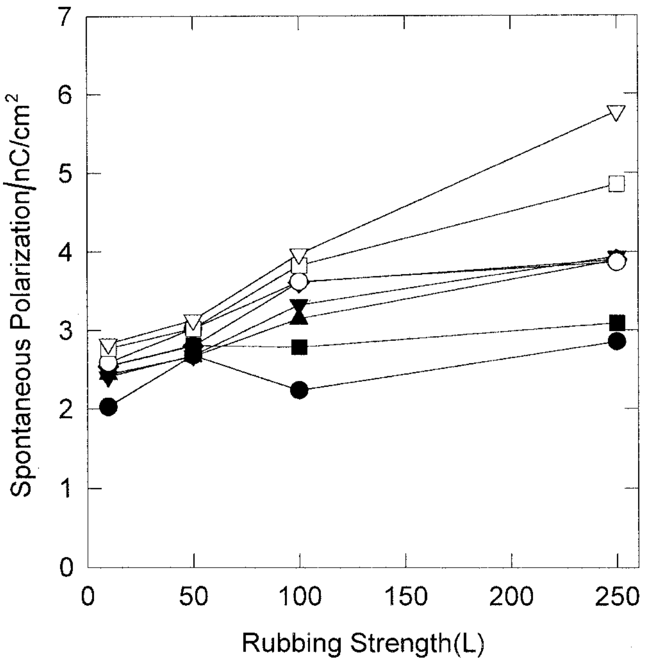

Figure 10. Dependence of spontaneous polarization on rubbing strength for a 2 μm cell at 25°C; ● 5, ■ 6, ▲ 7, ▼ 8, ◆ 9, ○ 10, 15, ▽ 20 $V_{p\text{-}p}$.

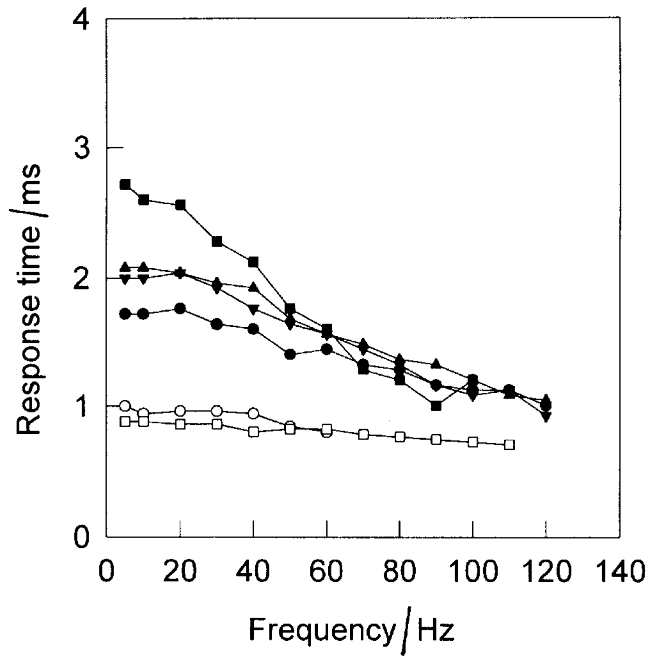

Figure 11. Dependence of response time on frequency for a 2 μm thick cell at 25°C; ■ LB (5 mN m^{-1}), ▲ LB (15 mN m^{-1}), ▼ LB (25 mN m^{-1}), ● LB (35 mN m^{-1}), ○ rubbing ($L = 150$), rubbing ($L = 250$).

3.4. *The effect of frequency and field on response time*

The fast response of a FLCD may come from the azimuthal motion on the cone in a tilt angle. The motion can be more easily induced in a low effective viscosity [14]. The response time for FLCs with different surface conditions (various LB and rubbed PI films) were measured by the field reversal method [10]. Its frequency dependence was measured by applying a 10 $V_{p\text{-}p}$ square pulse at room temperature. Figure 11 shows the response times of cells prepared under different conditions. At high frequency the response time was significantly reduced, but the presence of a depolarization field was shown at lower frequencies. This may be attributed to the accumulation of excess ions on the interfaces between the FLC medium and the alignment layer [18]. This residual ionic field lowers the effective field and reduces the switching speed. The switching of FLCs on the LB PI film becomes faster as the deposition surface pressure increases, perhaps because of the overall spontaneous polarization. In the preceding result, the overall spontaneous polarization increased as the deposition pressure and the rubbing strength increased. The switching speed is proportional to the inverse of spontaneous polarization as follows [13]:

$$t_r = \eta / (\mathbf{P}_s \ \mathbf{E})$$

where t_r is the response time, η is the reorientational viscosity, $\mathbf{P}_S$ is the spontaneous polarization, and $\mathbf{E}$ is the magnitude of the electric field.

Figure 12 shows the dependence of response time on the applied voltage. The 20 Hz square wave was applied at room temperature. The response time showed a maximum value near 5 $V_{p\text{-}p}$, decreasing proportionally to the electric field and spontaneous polarization. However, a remarkable phenomena occurred at lower voltage where a full switching might not be expected. A portion of FLC in a stable state needs a high field for switching; it is supposed that the fast response time at low field may be attributed to an easily switchable FLC.

3.5. *Memory time and transmittance*

Another feature of FLCs is bistability [19], which derives from two stable positions on the cone. A field is not needed to preserve FLC molecules in the switched state but only to switch them to the other state. However, bistability does not exist in the FLC mixture in this experiment, perhaps because of the presence of the depolarizing field arising from the ionic effects of impurities in the mixtures [18]. The LB films have a fairly good conductivity due to hopping conduction or electron tunnelling which may contribute to the discharge of the accumulated surface charges during the switching process [3]. Therefore, it is expected that these films will exhibit a long memory time. The decay time was measured by applying a 10 Hz, 20 $V_{p\text{-}p}$ biased square pulse wave with a pulse width of 20 ms. Figure 13 shows results for decay times on the different alignment layers.

The memory time on the PI LB film was longer than that on the rubbed film, while the cell fabricated at high deposition pressure had the shorter time.

Light transmission is an important factor in evaluating the feasibility of a display panel. Figure 14 shows the transmission obtained by measuring the maximum and minimum intensities of transmitted light during switching under applied fields. The light transmission of the FLC on the LB film is less than on the rubbed film, but the transmission of cells with PI LB films prepared at 25 or 35 mN m^{-1} deposition pressure approaches close to that of the rubbed film. The transmissions of the cells with PI LB films prepared at 5 and 15 mN m^{-1} are poor because of poor alignment of the FLC.

4. Conclusion

The monolayer and transfer characteristics of PMDA-3,3′-ODA PAAS at the air–water interface, and the alignment of FLCs on its LB film, have been studied. PAAS formed a stable monolayer and its transfer onto an ITO-coated glass substrate was better at a high surface pressure than at a low surface pressure. The closely packed state deposited forming a Y-type structure up to 11 layers, while the loosely packed state transferred with the Z-type arrangement. On a Si wafer, polarizing FTIR spectroscopy indicated that molecules on the wafer were oriented along the dipping direction. The roughness of LB films on the Si wafer decreased as the number of

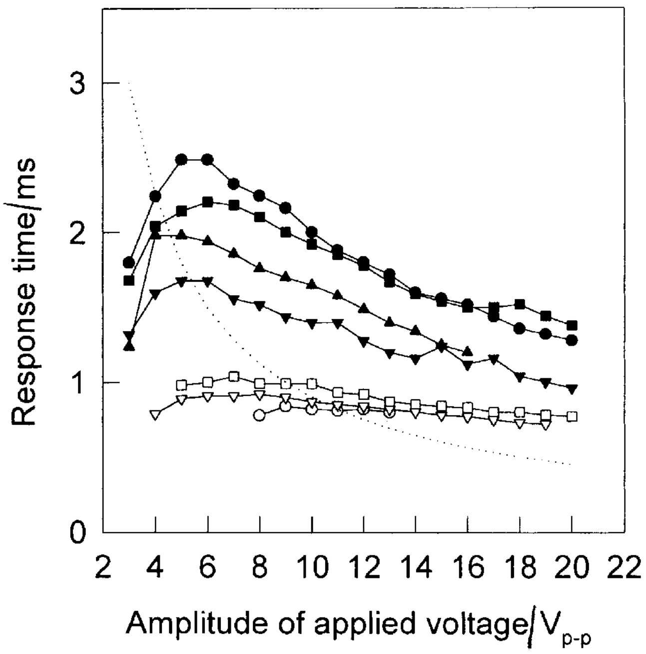

Figure 12. Dependence of response time on applied voltage for a 2 μm thick cell at 25°C; ■ LB (5 mN m^{-1}), ▲ LB (15 mN m^{-1}), ▼ LB (25 mN m^{-1}), ● LB (35 mN m^{-1}), ○ rubbing ($L = 10$), rubbing ($L = 150$), ▽ rubbing ($L = 250$); dashed line represents theoretical value.

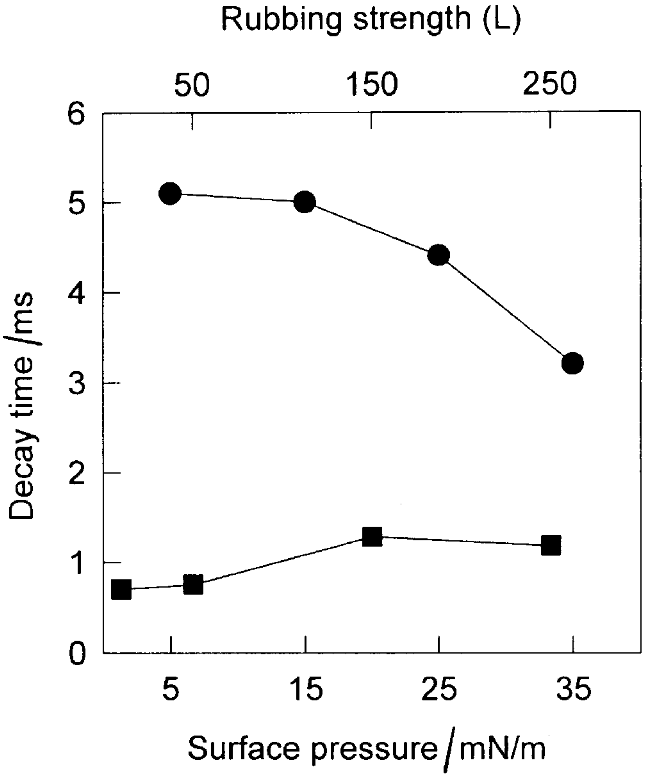

Figure 13. FLC decay time on different surfaces for a 2 μm thick cell at 25°C; ● PI LB film, ■ rubbed PI film.

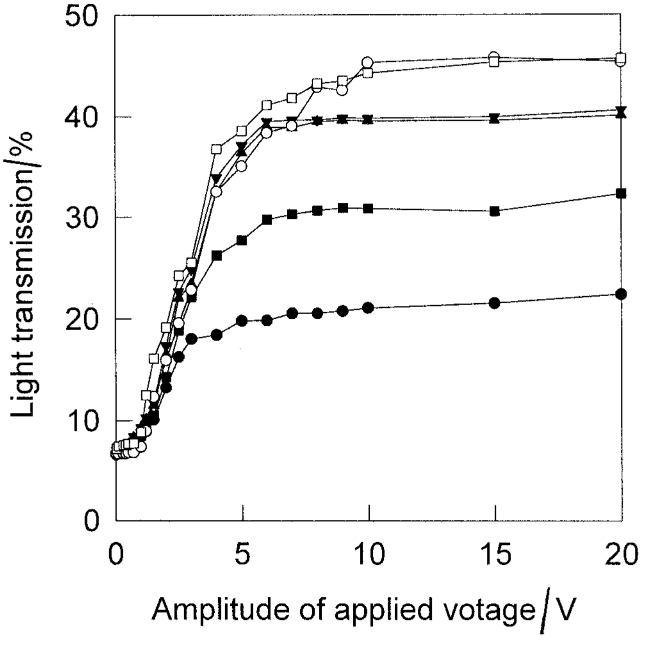

Figure 14. Light transmission of 2 μm thick FLC cells at 25°C; ● LB (5 mN m^{-1}), ■ LB (15 mN m^{-1}), ▲ LB (25 mN m^{-1}), ▼ LB (35 mN m^{-1}), ○ rubbed ($L = 150$), rubbed ($L = 250$).

layers increased. As the curing temperature increased, so did contact angles, and the surface became hydrophobic.

The well aligned FLC structure shows high spontaneous polarization. The low cooling rate and low thickness of the cell resulted in good alignment and high spontaneous polarization. The response time of an FLC under an external field also reflects the alignment state. At low frequency, ionic impurities in the mixture may generate a depolorization field and reduce the effective field. However, no significant ionic effect was observed in the region above 120 Hz. The decay time of the FLC decreased with decreasing spontaneous polarization. The LB film with a weak anchoring force showed a little slower response and longer decay than did the rubbed film; both showed nearly equivalent light transmission.

This work was supported by grant no. 1999-2-308-005-3 from the interdisciplinary research program of the KOSEF and also partially supported by the Brain Korea 21 Project.

References

[1] Murata, M., Uekita, M., Nakajima, Y., and Saitoh, K., 1993, *Jpn. J. appl. Phys.*, **32,** L679.

[2] Janning, J. L., 1972, *Appl. Phys. Lett.*, **21,** 173.

[3] Ikeno, H., Ohsaki, A., Nitta, M., Ozaki, N., Yokoyama, Y., Nakaya, K., and Kobayashi, S., 1988, *Jpn. J. appl. Phys.*, **27,** L475.

[4] Yokoyama, H., and van Sprang, H. A., 1985, *J. appl. Phys.*, **57,** 4520.

[5] Kimura, M., Nishikawa, M., Akahane, T., and Kobayashi, S., 1994, *Jpn. J. appl. Phys.*, **33,** L949.

[6] Kim, S. M., Koo, Y. M., and Kim, J. D., 1997, *Polymer Surfaces and Interfaces: Characterization, Modification and Application*, edited by K. L. Mittal and K. W. Lee (Utrecht: VSP), pp. 283–294.

[7] Tae, G. Y., Kim, S. M., Koo, Y. M., and Kim, J. D., 1995, *Mol. Cryst. liq. Cryst.*, **267,** 157.

[8] Kim, S. M., and Kim, J. D., 1996, *Mol. Cryst. liq. Cryst.*, **287,** 229.

[9] Miyasato, K., Abe, S., Takezoe, H., Fukuda, A., and Kuze, E., 1983, *Jpn. J. appl. Phys.*, **22,** L661.

[10] Bawa, S. S., Biradar, A. M., and Chandra, S., 1986, *Jpn. J. appl. Phys.*, **25,** L446.

[11] Tae, G. Y., Kim, S. M., Koo, Y. M., Kim, J. D., and Lee, K. J., 1995, *Synth. Met.*, **71,** 2097.

[12] Sakamoto, K., Arafune, R., Ito, N., Ushioda, S., Suzuki, Y., and Morokawa, S., 1996, *J. appl. Phys.*, **80,** 431.

[13] Patel, J. S., and Goodby, J. W., 1987, *Mol. Cryst. liq. Cryst.*, **144,** 117.

[14] Goodby, J. W., 1991, *Ferroelectric Liquid Crystals: Principles, Properties and Applications*, edited by G. W. Taylor (Amsterdam: Gorden and Breach), pp. 99–247.

[15] Kai, S., Nomiyama, M., Takahashi, T., and Imasaki, M., 1987, *Jpn. J. appl. Phys.*, **26,** L1831.

[16] Yamada, Y., Yamamoto, N., Mori, K., Nakamura, K., Hagiwara, Y., Suauki, Y., Kawamura, I., Orihara, H., and Ishibashi, Y., 1990, *Jpn. J. appl. Phys.*, **29,** 1757.

[17] Lee, E. S., Vetter, P., Miyashita, T., and Uchida, T., 1993, *Jpn. J. appl. Phys.*, **32,** L1339.

[18] Yang, K. H., and Chieu, T. C., 1989, *Jpn. J. appl. Phys.*, **28,** L1599.

[19] Clark, N. A., and Lagerwall, S. T., 1980, *Appl. Phys. Lett.*, **36,** 899.